Journal of Alloys and Compounds 382 (2004) 244–251

Journal of ALLOYS AND COMPOUNDS

www.elsevier.com/locate/jallcom

Application of positron annihilation techniques for semiconductor studies

G.P. Karwasz [a,*], A. Zecca [a], R.S. Brusa [a], D. Pliszka [b]

[a] *INFM and Dipartimento di Fisica, Universita' di Trento, via Sommarive, 14, Trento 38050, Italy*
[b] *Institute of Physics, Pedagogical University of Słupsk, Arciszewskiego 22B, Słupsk 76-200, Poland*

Received 21 October 2003; received in revised form 6 January 2004; accepted 19 January 2004

Abstract

Positron annihilation techniques, being non-destructive, allowing depth profiling down to a few micrometers and detecting open-volume defects (vacancies, dislocations etc.) at single ppm concentrations constitute a valuable and complementary method, compared to other solid-state-physics studies. We give examples of investigation in the field of semiconductors with different techniques, both with and without use of positron low-energy beams. The Doppler broadening of the 511 keV annihilation line method and the slow positron beam were used to study helium-implanted silicon and the surface reduction processes in semiconducting glasses. The positron lifetime technique and coincidence spectra of the Doppler broadening were used for systematic studies of metals and semiconductors. Doppler-coincidence method was then used to identify the kinetics of oxygen precipitates in Czochralski-grown silicon.

Keywords: Semiconductors; Precipitation; Point defects; Positron spectroscopies; Positron annihilation; Silicon; Implantation; Helium

1. Introduction

Positron annihilation spectroscopies are non-destructive, depth resolved, highly defect-sensitive methods [1]. Advent of new, high intensity, narrow-spot positron beams [2] opens new possibilities for solid state spectroscopy. Annihilation techniques still maintain high complexity from the experimental point of view, therefore positron set-ups are less spread than for example the setup for optical spectroscopies.

Positrons have been predicted theoretically by P.A.M. Dirac in 1930 and then observed in cosmic radiation by Anderson in 1932 who used a specially constructed bubble chamber in a strong magnetic field and reported [3] "positive particles which could not have a mass greater as that of the proton". Free positron and electron can form positronium, i.e. hydrogen-like atom: if it is in a singlet (para-Ps) state, then, due to spin-conservation it annihilates via a 2-γ decay, with 125 ps lifetime; in a triplet state positronium (ortho-Ps) survives 142 ns and annihilates in a 3-γ decay. Nowadays, positrons can be obtained from artificial radio-nuclides, like ^{22}Na, ^{58}Co etc. Another way of obtaining positrons is the pair creation from high-energy gamma-rays generated in bremstrahlung of electrons with energy in MeV range.

In solid state, positrons emitted from (radioactive) sources slow down by inelastic collision to thermal energies in less than 10^{-12} s, then diffuse and annihilate with electrons of the medium. The positron annihilation, due to the light mass of e^+ and the low e^+ current is a non-destructive technique. Additionally, positrons are especially sensitive to vacancy-like defects in solids—the lack of positive charge (a removed ion) in such defects forms a local, negative potential, attracting positrons. The diffusing positron is therefore attracted by open volume defects and annihilates preferentially there, see Fig. 1. As the de Broglie's wavelength of positrons at room temperatures is about 20 Å, the thermalized positron "sees" contemporarily a big portion of the solid—its sensitivity to vacancy-like defects is of 1 ppm order.

2. Positron annihilation spectroscopies

γ-Quanta originating from annihilation events bring information on the total momentum of the pair—i.e. essentially of the electron (positron energy is of 25 meV order). Broadening of the 511 keV annihilation line was observed already in early research [4]. DeBenedetti et al. [5] were first

* Corresponding author.
E-mail address: karwasz@science.unitn.it (G.P. Karwasz).

0925-8388/$ – see front matter © 2004 Elsevier B.V. All rights reserved.
doi:10.1016/j.jallcom.2004.05.037

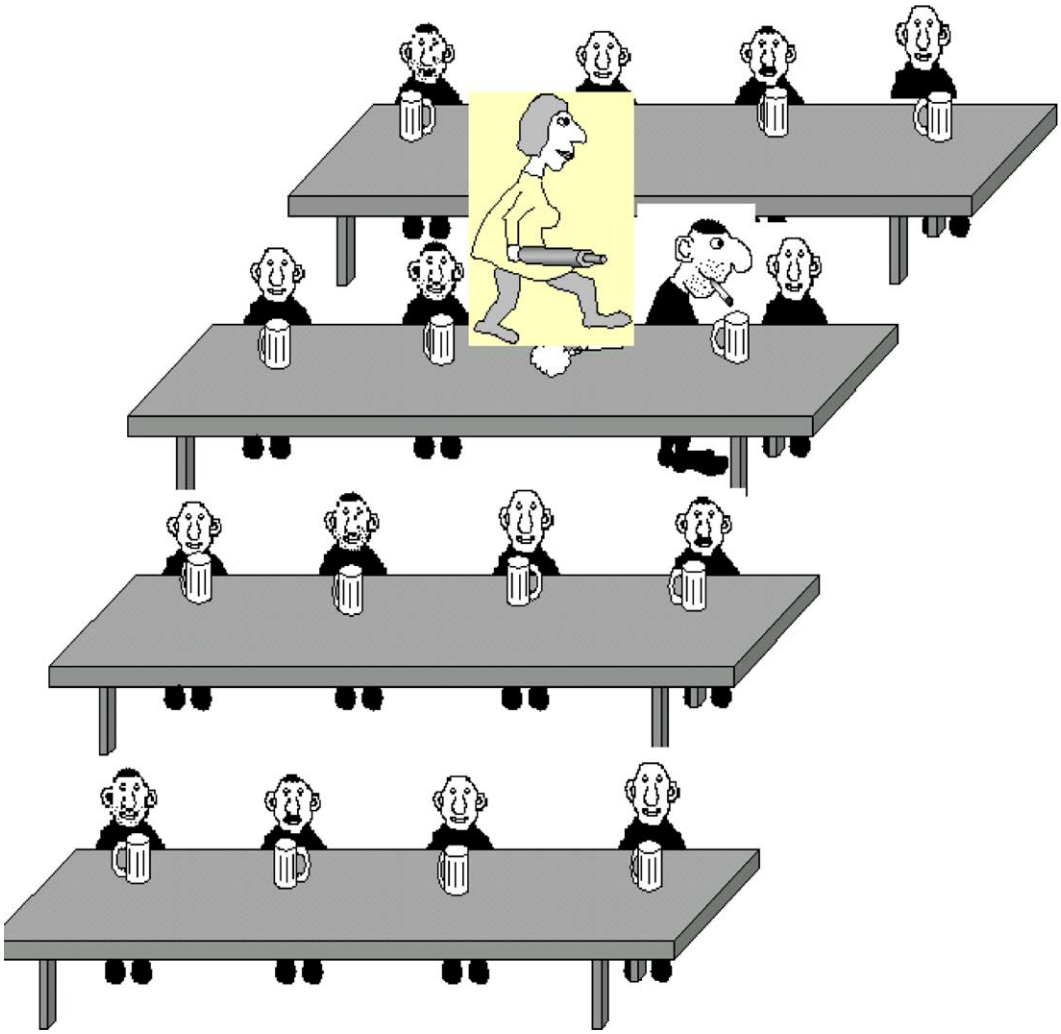

Fig. 1. Drawing illustrating a high sensitivity of positrons to vacancy-like defects—a positron (she) searching for an atom (he) lacking from its position in a prefect crystal. The positron, walking inside the solid, constitutes a thermal-energy de Broglie wave (about 20 Å wavelength) and is attracted by an atomic vacancy (the lack of the positive charge of the ionic core is an attractive potential for positrons) and finally annihilates there. [The drawing is courtesy of Dr. Tomasz Wróblewski].

to notice that two 511 keV γ-rays originating from positronium annihilation with electrons in solid state do not form exactly 180°—as the momentum of thermal positrons is almost zero compared to momentum of 511 keV photons, this shift is to be attributed to momentum of the electron with whom the positron annihilates. This observation initiated studies of electron momenta by angular correlation of annihilation radiation (ACAR) method. The utility of ACAR method is mainly used to the determination of Fermi surfaces in single-crystal metals and alloys, see for example [6]. In order to obtain a high angular resolution long distances between detectors are needed and therefore the coincidence signal from the two γ-rays originating from the annihilation event is low.

The second method used is the positron lifetime technique. In defect-free solids, the lifetime of positrons depends on the kind of chemical element, as shown for selected examples in Table 1. These lifetimes, for elements like V, Ni, W are close to 100 ps, so fast photomultipliers are used. A scheme of positron lifetime experiment is given in Fig. 2. As a start signal the prompt γ from radioactive decay is used (for example, the 1275 keV one for the ^{22}Na source), as a stop one—the 511 keV γ. Practically, due to possible Compton scattering of γ-quanta before reaching scintillators, somewhat wider (towards lower energies) windows are used for both start and stop signals.

In presence of vacancy-like defects, the lifetime of positrons rises because the electronic density in the region of vacancies is lower than in the bulk. Positrons trapped in different types of defects have different lifetimes.

The third type positron-annihilation spectroscopy is the Doppler-broadening technique, see Fig. 3. It measures the projection p_L of electron momentum on the direction of observation, this quantity is related to the observed broadening ΔE of the 511 keV line through the relation $p_L/m_0c = 2\Delta E/E$. By measuring the Doppler-broadening

Table 1
Measured lifetimes for some elements, relevant to semiconductor technologies

Z	Element	τ_{exp}	τ_{th} [9]	τ_{th} [20]
5	Be	209	–	
13	Al	160	166	163.3
14	Si	220	221	217.0
22	Ti	145	146	
23	V	123	116	129.8
28	Ni	105	96	112.1
29	Cu	115	106	122.8
32	Ge	227	228	
40	Zr	159	159	
74	W	115	100	
79	Au	206	187	120.3

Given: the atomic number Z, experimental [7,8] and theoretical [9,20] (BN-WDA model) approximation lifetimes (in ps). Experimental lifetimes in some cases, like Cu and Au are average lifetimes over two components. In presence of vacancy-like defects, the lifetime rises—the electron density in vacancies is lower than in the bulk and therefore the annihilation probability is also lower. For example, in W, difficult to anneal, we have measured two lifetime-components, 103 ps in a perfect agreements with the theoretical value, and 244 ps (with 9% intensity). Positron trapped in a defect has a lifetime characteristic of that type of defect. For example, the lifetime in single vacancies in Si is 250 ps and in bi-vacancies 270 ps [10].

one gets a one dimensional distribution of momentum of the positron-electron annihilating pairs. More precisely, two parts in the Doppler-broadening spectrum can be distinguished: a low momentum distribution part (valence and conductivity electrons) and high momentum part ("core" electrons, tail of the spectrum), see [11].

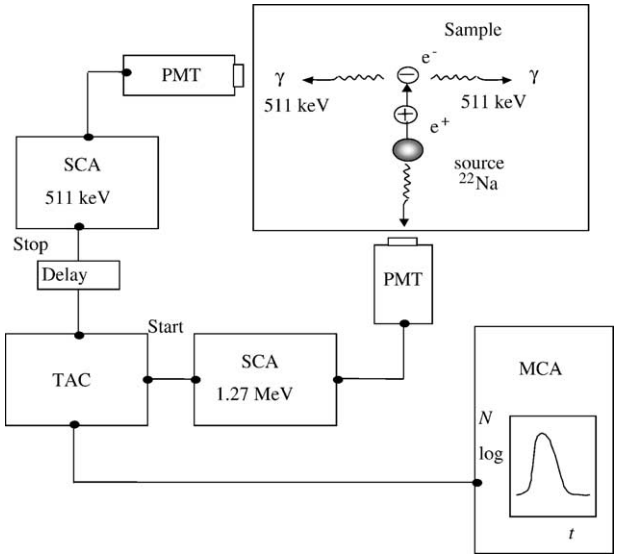

Fig. 2. Scheme of positron annihilation lifetime apparatus. The studied material is put into a sandwich formed by the source (e.g., ^{22}NaCl salt) and two identical samples. The γ signals (the start one from radioactive decay and the stop one of the 511 keV annihilation line) are detected by scintillators coupled to fast photomultipliers. The electronic circuitry measures the number of events vs. the delay time between the start and stop signals.

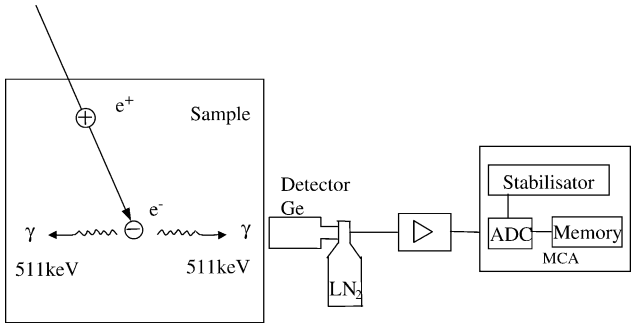

Fig. 3. Scheme of Doppler-broadening measurements. Only one of the γ annihilation quanta is detected and analyzed in energy. High purity Ge detector and special spectra stabilization procedures are used.

To study positron annihilation with valence electrons, the so-called shape parameter "*S*" is used. The *S*-parameter is defined as the ratio between the number of counts in the central part of the $E_0 = 511$ keV broadened line to the total counts in the spectrum, i.e. as S = [number of counts in $(E_0 \pm 0.85\,\text{keV})$]/[number of counts in $(E_0 \pm 4.25\,\text{keV})$] in our measurements. The central part of the spectrum corresponds to low-energy, i.e. valence electrons. The rise of the *S*-parameter corresponds to an increasing number or/and increasing size of vacancy-like defects in the solid (Fig. 4).

The weak point of *S*-parameter measurements is that it does not allow to determine the chemical surroundings of the annihilation site. The coincidence technique (Fig. 5) allows to lower the background and to measure the high momentum part of the spectrum (Fig. 6).

For example, in Trento measurements two detectors in a collinear geometry are used, Fig. 4. The main detector was a high purity germanium detector (HPGe) with 16%

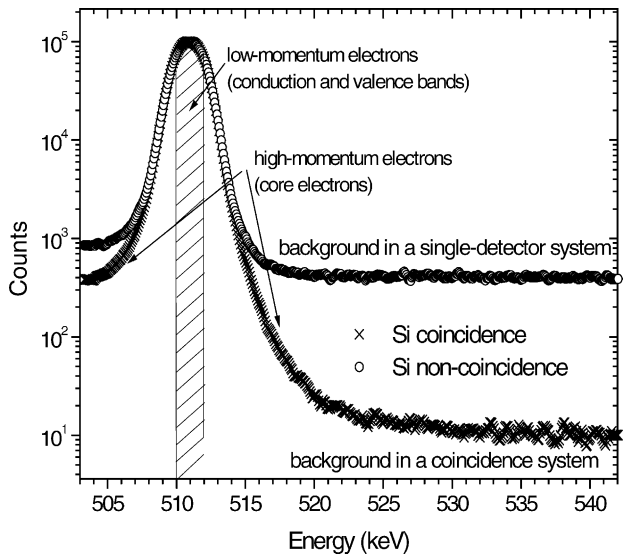

Fig. 4. The scheme of Doppler broadening measurements in coincidence. Two detectors at 180° angles are used, at least one of which (high purity germanium) measures the energy spectrum of annihilation γ-quanta. In present measurements the second detector was a sodium iodide scintillator.

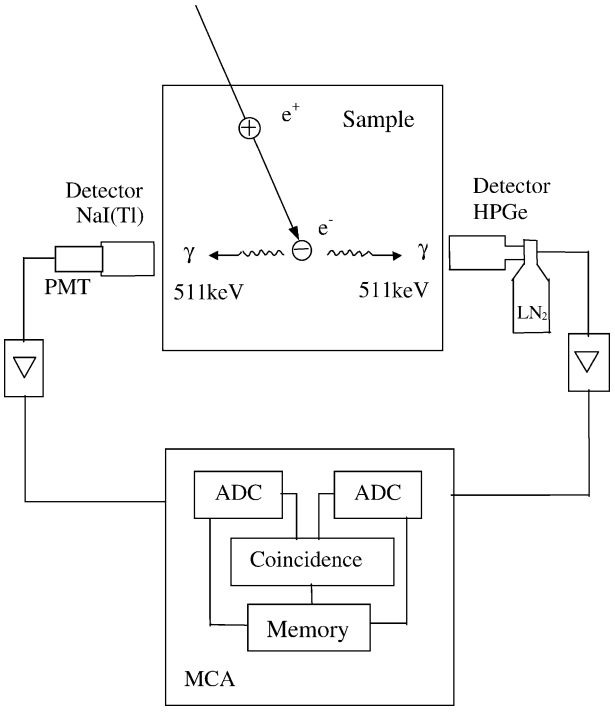

Fig. 5. Shape of the typical annihilation line. Note lowering of the background level with the use of the coincidence technique.

efficiency and energy resolution 1.3 keV (at the 511 keV annihilation line). The second detector was a (NaI)Tl scintillator. The use of coincidence technique allows to study chemical surrounding of defects because every element has a specific "fingerprint" in annihilation spectrum. In order to

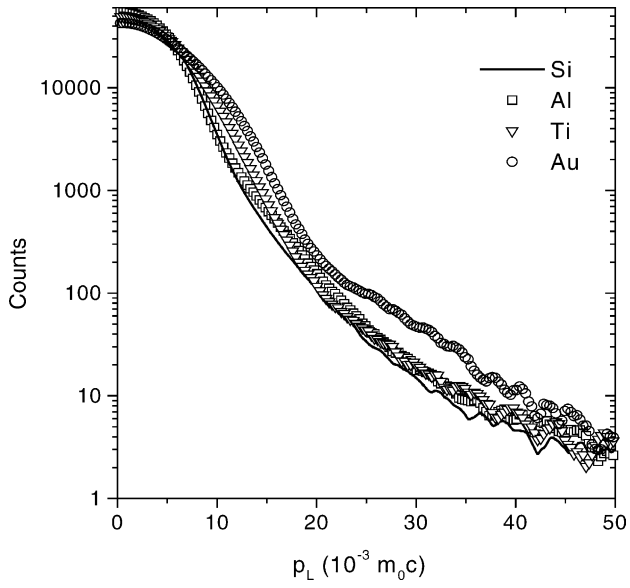

Fig. 6. Examples of 511 keV annihilation line shapes obtained with the coincidence technique: note the low noise (essentially due to spure cosmic radiation and radioactivity of construction material) in the high energy tail of the spectrum. Note also that relative differences between the spectra for different elements are small and therefore some normalization techniques (for example by referring to low-Z material, like Si or Al) are needed.

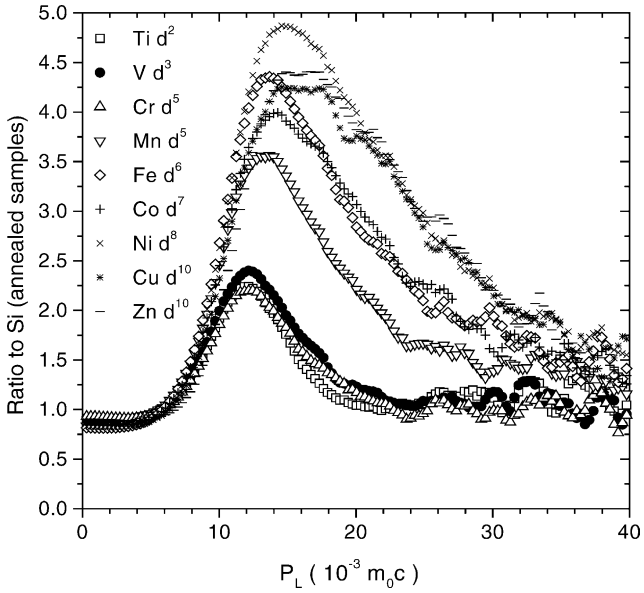

Fig. 7. Examples of Dopper broadening annihilation curves of selected atomic elements referred to the annihilation line in p(1 0 0) single-crystal silicon, data from Trento laboratory.

evidence slight differences in the 511 keV annihilation lines for different elements, usually ratio curves are used, in reference to some light element, like Al [9] or Si [10], see Fig. 7.

Fast positrons emitted from radioactive sources penetrate into solid with a depth profile extending down to several tenth of millimeter (for example 99% of them is stopped in 1 mm layer in case of Si). In order to obtain depth-resolved parameters of annihilation, positrons have to be slowed down first and then implanted into the sample with controlled energy. Beams of controlled energy are rather simple to construct if Doppler-broadening is studied [12] but become more complex if lifetime depth profiles are needed [13].

The Trento low-energy positron beam for Doppler-broadening studies is shown in Fig. 8. Positrons emitted from the ^{22}Na source are implanted into a thin (1 μm) W monocrystal, they slow down inside W and then are re-emitted with about 2 eV kinetic energy from the other side of the monocrystal. Slow positrons are then guided by electrostatic optics and implanted into the sample with the energy adjustable between 50 eV and 25 keV with a beam spot from 4 to 1 mm diameter. A high-purity Germanium detector is positioned below the sample, outside the vacuum system. Details of the set-up have been given elsewhere [12].

3. Applications to semiconductor studies

The first case study for semiconductors is an example of Doppler broadening measurements in He-implanted silicon [14]. The technological need for such measurements is that nano-cavities formed after thermal treating of implanted

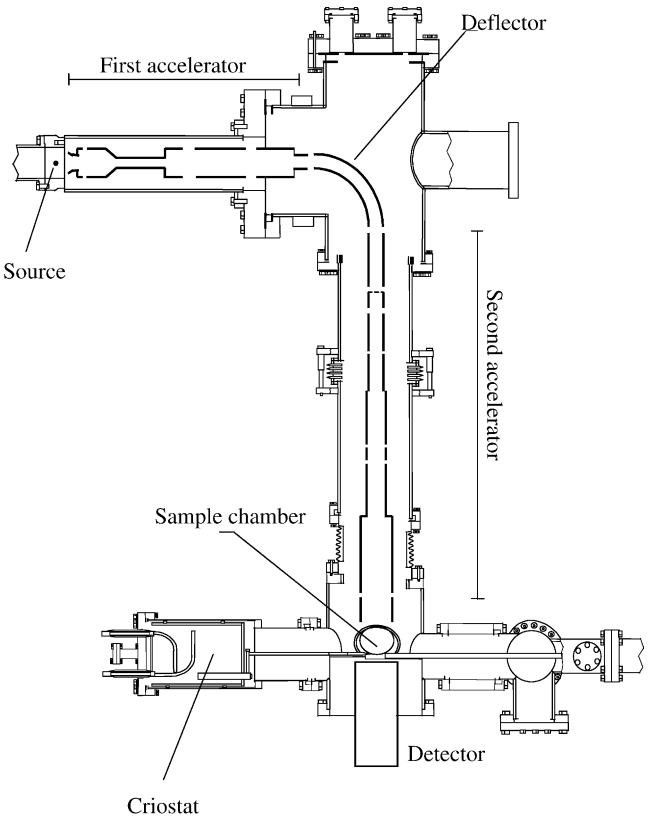

Fig. 8. The scheme of Trento slow-positron beam apparatus. Fast positrons from the radioactive source are slowed down in the moderator, the re-emitted beam is accelerated by the first part of optics, than bent by 90° (in order to eliminate residual fast positrons), accelerated to the desired implantation energy and injected into the sample. The lower part of the apparatus contain a manipulator and a cryostat for the sample.

samples serve as gathering volumes for numerous impurities in silicon or for smart-cut technologies. A specific goal of present measurements was to identify why the low implantation doses ($0.5 \times 10^{16}\,cm^{-2}$) do not lead to formation of any cavities and higher doses ($2.0 \times 10^{16}\,cm^{-2}$) lead to formation of pretty big cavities (of 10–50 nm diameters).

In Fig. 9 we show the *S*-parameter measurements for three samples: in the reference sample (defect free Si) the *S*-parameter, normalized to bulk *S* value, rises smoothly from a value typical for the surface to the value of 1.0 in bulk. In He-implanted sample its rise above 1.0 indicating the presence of vacancy-like defects for a given depth. We have shown [14] that during the thermal treatment below 450 °C, the *S*-signal rises with rising the temperature of annealing for both implantation doses. Then, above 450 °C, for high doses ($2 \times 10^{16}\,cm^{-2}$) the "S" signal continue to grow up showing the formation of nanovoids around 200 nm depth, see Fig. 9b. On the contrary, vacancies-like defects disappear above 450 °C in low implantation dose ($5 \times 10^{15}\,cm^{-2}$) samples.

A second example of positron-annihilation applications is the tracing of open volume defects associates to oxygen precipitates in Czochralski-grown silicon [15]. Oxygen is

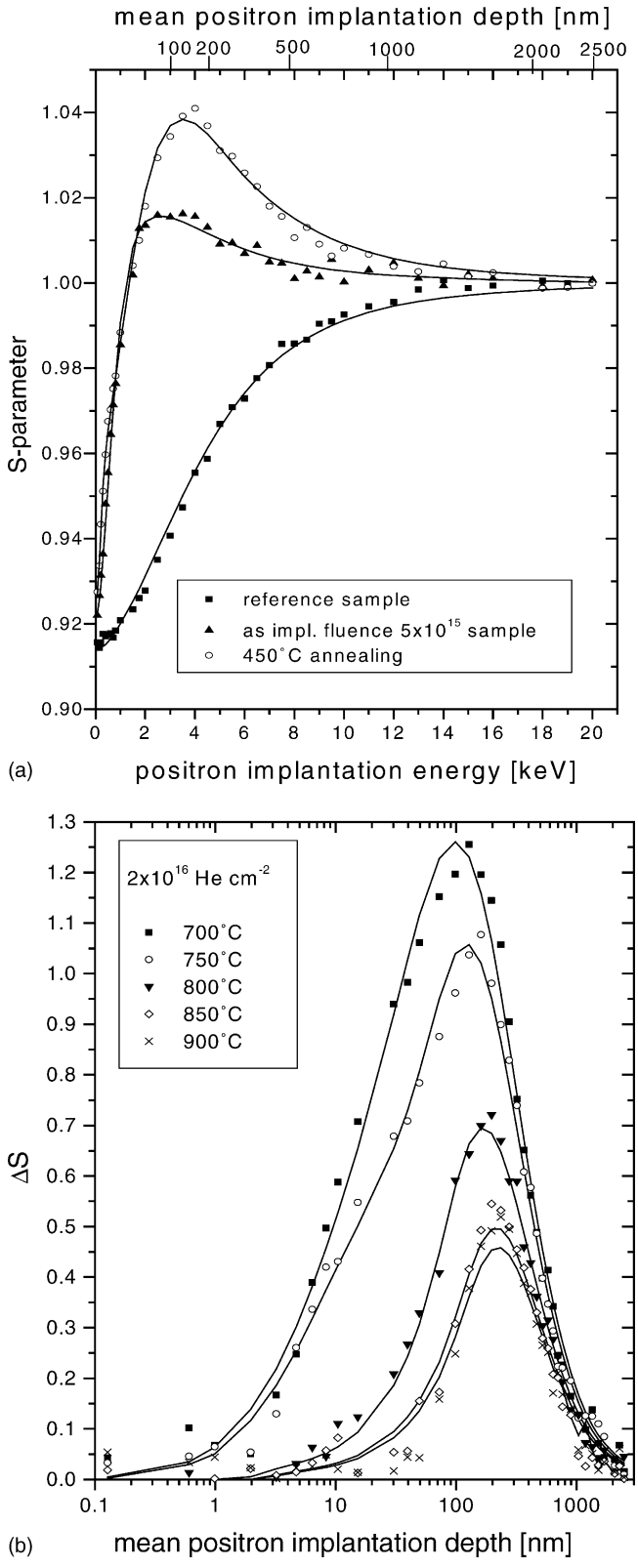

Fig. 9. S-parameter in He-implanted silicon. (a) Experimental curves normalized to bulk silicon. (b) Relative curves: difference with the curve of the reference silicon, after annealing at different temperatures, from [12]. The curves of (b) indicates the variation in the size of the active positron traps and their localization.

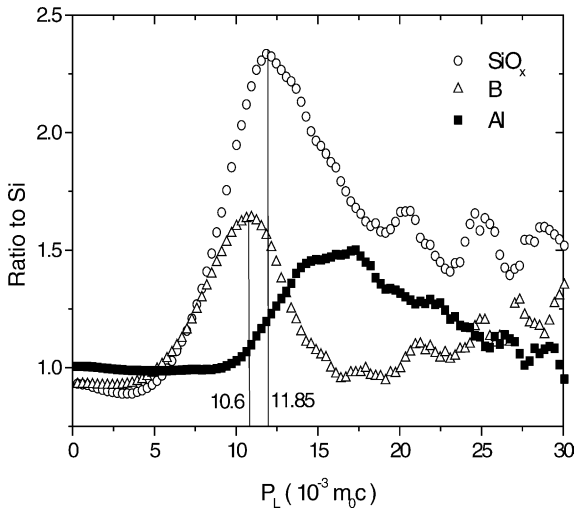

Fig. 10. Doppler-broadening annihilation spectra obtained by the coincidence technique-ratios to Si spectra. Peaks originating from oxygen, boron and aluminum can be identified.

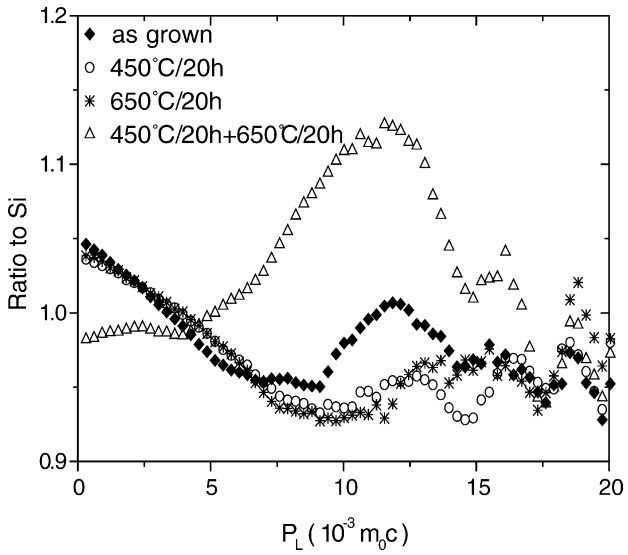

Fig. 11. Doppler coincidence investigations of Czochralski-grown silicon with high oxygen-contents. Lowering of the coincidence parameter in samples annealed at 450 °C indicates migration of oxygen atoms from defect sites to interstitial positions. This type of annealing is a standard recipe of semiconductor industries, used for "as-grown" samples, in order to remove the electrical activity of oxygen atoms. That recipe was purely phenomenological and positron annihilation studies [15] allow to explain it.

unavoidable impurity in Si, added just in the final process, i.e. monocrystal are grown in quartz crucibles. The contents of O-atoms exceed by one to two orders of magnitude the contents of dopants, therefore oxygen could prevail in determining semiconductor properties of silicon. It is well-known from the beginning of silicon era, that prolonged thermal treating at about 450 °C removes the electrical activity of O-atoms [16]. However, the exact dynamics of O-atoms during such thermal treating was not known. It was also (phenomenologically) known that additional heating at 650° re-introduces donor activity but the reasons were not clear. Finally, treatments at 800–900 °C after preliminary heating at 450 and 650 °C lead to formation of oxygen precipitates.

In Fig. 10 we present Doppler-broadening coincidence curves obtained as ratio of 511 keV annihilation profiles for the given element to the shape of annihilation line in a high-purity, defect free, low-oxygen contents silicon. From this Figure one can deduce that a peak at about 11.85 $\times$ 10^{-3} m_0c^2 in our spectra is a fingerprint for oxygen presence.

In Fig. 11 we present Doppler-broadening coincidence ratio curves for sample of Czochralski-grown silicon with a high (11×10^{17} cm^{-3}) oxygen contents, annealed at different temperatures. As seen in Fig. 11, in as-grown silicon some traces of oxygen in defects are visible, majority of it remaining in interstitial position, i.e. being partially "invisible" for positrons. From the positron-annihilation signal in Fig. 11 one can deduce that heating at 450 °C removes all oxygen to interstitial positions, making it also inactive electrically. A two-step heating, at 450 and 650 °C makes the oxygen well visible to positrons, creating probably small nucleation centers (a few oxygen atoms around a defect) for further oxygen precipitates [16]. As shown in detail in [15], the Doppler-broadening positron-annihilation coincidence curves allow to follow also those steps.

Another technological problem deal with our positron annihilation studies was to determine an optimal thermal treatment in semiconducting glasses used as image amplifiers [17,18]. These materials are usually silica glasses doped with lead oxides. The reduction treatment in H_2 atmosphere reduces the lead oxides on the surface to a metallic phase,

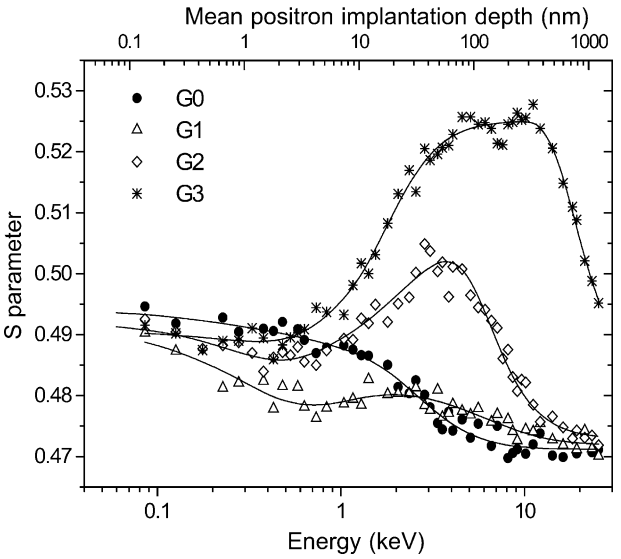

Fig. 12. Reduction processes in bismuth-germanate glasses heated at 340 °C for a variable time, from 45 min (G1) to 7 h (G3). "G0" is as-obtained glass. Tracing the "valence" annihilation S-parameter allows to determine optimum thermal treatments for the desired reduced depth. Glasses are used for electron-multipliers and image-intensifiers.

making the glass conducting on the surface. However, it is also required to maintain a high resistivity in the bulk, therefore controlling of the reduction depth is crucial in the whole process.

In a series of works we used slow positron beam for studies of different types of glasses, based on silicon or germanium oxides and doped with lead or bismuth oxides. In all non reduced glasses the Doppler broadening *S*-parameter is low, like at the surface (i.e. oxidized) state of silicon, compare Fig. 9. The reduction in hydrogen atmosphere rises the *S*-parameter. Our measurements, like those shown in Fig. 12, allow to trace the depth of the reduced layer, showing how it moves inside material with prolonged treatments and to choose the optimal treatment.

Finally, in Fig. 13 we present studies of low-ε thin films of SiCOH layer (3400 Å) deposited on silicon substrate treated in N_2 (400 °C, 30 min) and then treated in N_2 plasma (450–900 °C for 30 min in vacuum) in order to produce a capping layer at the surface. The dielectric constants of the dielectric layer is $\varepsilon = 2.9$. The presence of nanopores was traced by 3-γ positron annihilation measurements, monitoring so-called PV ("valley") parameter—a relative number of γ quanta in the range $100\,\text{keV} \leq E_\gamma \leq 450\,\text{keV}$ compared to the total number of γ in the annihilation peak 511 ± 4.25 keV. Curves in Fig. 13 indicate clearly presence of large open-volume space at the depths of about 100 nm. During ageing the material in air, these pores become invisible for positrons, probably gas-filled. A prolonged (48 h) heating in high vacuum makes these cavities turn to the original (as seen by positrons) state. Further work on this subject is in progress [19].

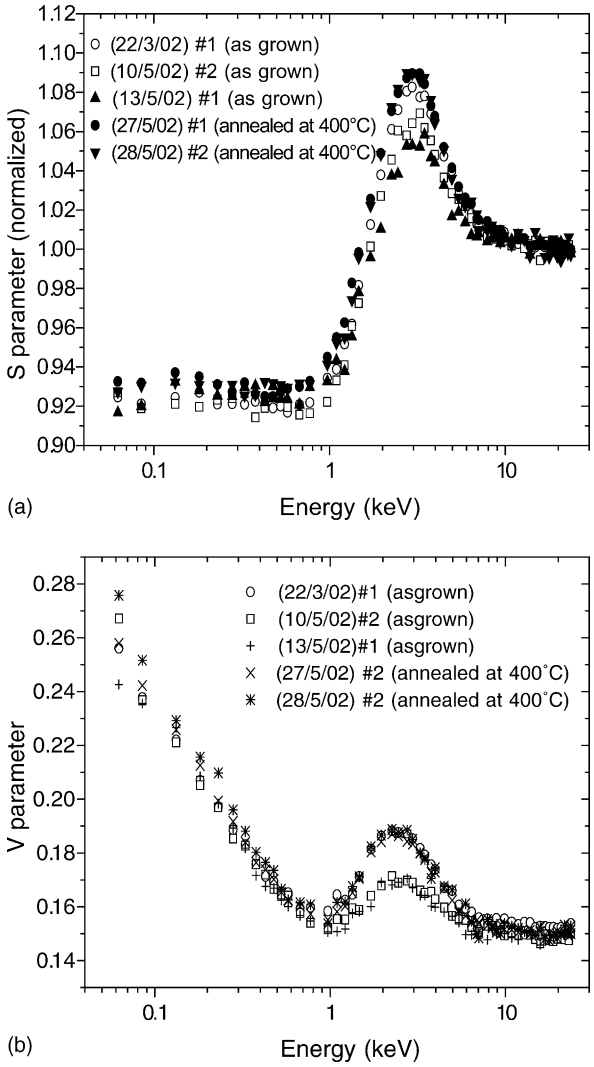

Fig. 13. Aging of high-porosity, low-ε, materials, due to filling of pores by atmospheric gases. The lowering of positron "3-γ" annihilation events indicated reductions of free-volumes inside the material. The positron spectroscopy reveals that this processes is fully reversible, if an adequate annealing is applied.

4. Conlusions

We have illustrated, how combined positron-annihilation techniques can be applied to several problems of semiconductors technologies. In the case of He-implanted silicon, the use of the positron beam with the adjustable energy (from 100 eV to 25 keV) allowed to follow the dynamics of defects leading to formation of nano-cavities. For the high dose of He ($2 \times 10^{16}\,\text{cm}^{-2}$), vacancy-type defects enlarge with thermal treatments, passing from bi-vacancies to multi-vacancies and eventually to nano-voids [14]. To get these conclusions, the use of the "simple" Doppler-broadening technique was sufficient.

In the case of oxygen precipitates in Czochralski-grown silicon, the use of the simple Doppler technique and the positron lifetime technique was not sufficient. Only the application of the coincidence measurements to Doppler broadening allowed to follow the dynamics of the oxygen-related defects. At 450 °C oxygen atoms move to interstitial sites and are not more visible for positron; after 450 °C plus 650 °C combined treatment, the oxygen-related, defect-like centers appear, becoming next nucleation centers for oxygen precipitates.

In the case of semiconducting glasses, the positron beam allows to follow dynamics of the surface reduction processes, but the lack of the coincidence technique with a controlled positron implantation depth does not allow to identify precipitation sites for metal nano-grains. Once more, similarly to He-implanted silicon, the Doppler no-coincidence method is sufficient to trace gas filling in low-ε materials.

Acknowledgements

We thank Provincia Autonoma di Trento for partial support under the PPD-Carbon project.

References

[1] R. Krause-Rehberg, H.S. Leipner, Positron Annihilation in Semiconductors—Defect Studies, Springer Series in Solid-State Sciences 127, Springer-Verlag, Berlin, 1999.
[2] A. Zecca, G. Karwasz, Physics World, November 2001, pp. 21.
[3] C.D. Anderson, Science 76 (1932) 238.
[4] J.W.M. DuMond, D.A. Lind, B.B. Watson, Phys. Rev. 75 (1949) 1226.
[5] S. DeBenedetti, C.E. Cowan, W.R. Konneker, Phys. Rev. 76 (1949) 440.
[6] M. Biasini, G. Ferro, G. Kontrym-Sznajd, A. Czopnik, Phys. Rev. B 66 (2002) 075126.
[7] R.S. Brusa, W. Deng, G.P. Karwasz, A. Zecca, Nuclear Instr. Meth. Phys. Res. B 194 (2002) 519.
[8] W. Deng, D. Pliszka, R.S. Brusa, G.P. Karwasz, A. Zecca, Acta Phys. Pol. A 101 (2002) 875.
[9] M.J. Puska, R. Nieminen, Rev. Mod. Phys. 66 (1994) 481.
[10] M. Hakala, M.J. Puska, R. Nieminen, Phys. Rev. B 57 (1998) 7621.
[11] P. Asoka-Kumar, K.G. Lynn, D.O. Welch, J. Appl. Phys. 76 (1994) 4935.
[12] A. Zecca, M. Bettonte, J. Paridaens, G.P. Karwasz, R.S. Brusa, Meas. Sci. Technol. 9 (1998) 409.
[13] A. Zecca, R.S. Brusa, M.P. Duarte-Naia, G.P. Karwasz, J. Paridaens, A. Piazza, G. Kögel, P. Sperr, D.T. Britton, K. Uhlmann, P. Willutzki, W. Triftshäuser, Europhys. Lett. 29 (1995) 617–622.
[14] R.S. Brusa, G.P. Karwasz, N. Tiengo, A. Zecca, F. Corni, R. Tonini, G. Ottaviani, Phys. Rev. B 61 (2000) 10154.
[15] R.S. Brusa, W. Deng, G.P. Karwasz, A. Zecca, D. Pliszka, Appl. Phys. Lett. 79 (2001) 1492.
[16] A. Borghesi, B. Pivac, A. Sasella, A. Stella, J. Appl. Phys. 77 (1995) 4169.
[17] B. Kusz, D. Pliszka, M. Gazda, R.S. Brusa, K. Trzebiatowski, G.P. Karwasz, L. Murawski, J. Appl. Phys. 94 (2003) 7270.
[18] D. Pliszka, M. Gazda, B. Kusz, K. Trzebiatowski, G.P. Karwasz, W. Deng, R.S. Brusa, A. Zecca, Acta Phys. Pol. 99 (2001) 465.
[19] R.S. Brusa, M. Spagolla, G.P. Karwasz, A. Zecca, G. Ottaviani, F. Corni, E. Carollo, J. Appl. Phys. 95 (2004) 2348.
[20] A. Rubaszek, Z. Szotek, W.M. Temmerman, Phys. Rev. B 58 (1998) 11285.